

---

## Effect of Fire on Concrete Contribution to Shear Resistance of GFRP RC Beams

<https://www.doi.org/10.56830/IJSIE06202303>

**Mahmoud Mehany**

*Department of Civil and Building Engineering*

*University of Helwan, Cairo, Egypt*  
[eng.mahmoud.abdelghafar@gmail.com](mailto:eng.mahmoud.abdelghafar@gmail.com)

### **Abstract**

The use of fiber-reinforced polymer (FRP) bars is becoming commonplace in various civil engineering applications due to the several advantages they offer over traditional materials. However, limited knowledge about some aspects of the behavior of FRP bars, particularly when subjected to severe fires, is hampering their widespread use. This paper presents the results of a research program to investigate the shear behavior of glass-FRP (GFRP)-reinforced beams exposed to severe fires. Three reinforced concrete (RC) beam specimens with a cross-sectional width and height of 150 mm and 300 mm, respectively, and with a total length of 1700 mm were constructed and tested under four-point bending load up to failure. The main test variables were the reinforcement ratio and the fire. The experimental results show that all beams failed as a result of diagonal tension cracking. The shear resistance and stiffness of the RC beams decreased when the beams are exposed to fire at the same reinforcement ratio.

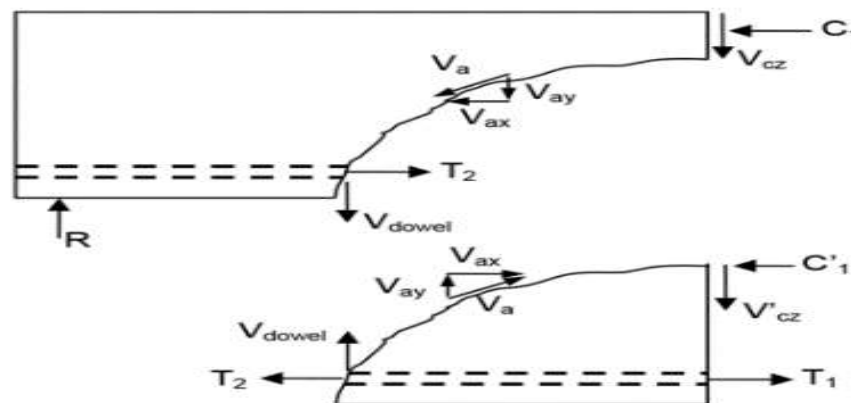
**Keywords:** *GFRP bars, reinforced concrete beams, fire, shear capacity, crack patterns, modes of failure.*

### **Introduction**

Nowadays, fiber-reinforced polymer (FRP) bars are being more accepted in many design codes ((CSA), 2012); (Canadian, 2019); (American, 2015) as an alternative reinforcement to conventional steel bars in reinforced concrete (RC) members. Among the different types of FRP bars, Glass-FRP (GFRP) bars are widely used as longitudinal reinforcement in North America due to their superior performance. In addition to its excellent corrosion resistance, GFRP reinforcement has a high strength-to-weight ratio, good fatigue properties as well as good resistance to chemical attack and electromagnetic resistance. GFRP bars can be used in concrete structural members such as foundations, breakwaters, and other structures subjected

to harsh environmental effects exhibit good resistances to chemical aggressiveness and fire.

Significant effort has been given in the last decades to study the behavior of FRP RC elements and to improve the design guidelines, especially the shear design equations. Current shear design provisions of FRP RC elements are based on experimental data mostly obtained from shear testing of RC beams. The concrete contribution to the shear resistance of the section represents the shear resisted by various shear mechanisms. ACI-ASCE Committee 445 (ASCE-ACI, 1998) assessed that the quantity of concrete shear strength can be considered as a combination of five mechanisms activated after the formation of diagonal cracks: (1) uncracked concrete, (2) aggregate interlock, (3) dowel action of the longitudinal reinforcement, (4) arch action, and (5) residual tensile stresses across the inclined crack (see Fig. 1). The contribution of the uncracked concrete in RC elements depends mainly on the concrete strength and on the depth of the uncracked zone, which is function of the longitudinal reinforcement properties.



where:

$R$  = reaction

$C_1, C'_1$  = compression forces

$T_1, T_2$  = tension forces

$V_{cz}$  = shear transferred in the uncracked concrete (flexural compression zone)

$V_a$  = interface shear transfer (aggregate interlock)

$V_{dowel}$  = dowel shear

**Fig (1) :** Internal forces in cracked beam without stirrups (MacGregor & Wight, 2005).

Generally, there is a paucity of the experimental studies regarding RC members reinforced with FRP bars under fire exposure (Nigro, G. Cefarelli, Bilotta, & Cosenza, 2011); (Hajiloo, Green, Noël, Bénichou, & Sultan., 2017); (Gooranorimi, Claire, De Caso, Suaris, & Nanni, 2018); (Hajiloo, H.; Green, M. F.; Noël, M.; Bénichou, N.; Sultan, M., 2019). (Nigro, G. Cefarelli, Bilotta, & Cosenza, 2011);

(Hajiloo, Green, Noël, Bénichou, & Sultan., 2017) showed that the bond failure of fire exposed GFRP RC slabs can be prevented by providing sufficiently long unexposed (cool) regions to ensure adequate anchorage of the bars. (Gooranorimi, Claire, De Caso, Suaris, & Nanni, 2018) exposed six small-scale 2000 mm long GFRP RC slabs to (ASTM., 2015) standard fire. The slabs were similar to each other with the exception of the surface treatments of the reinforcing bars; three of the slabs were reinforced with sand coated GFRP bars, and the other three slabs were reinforced with bars with surface deformations. The test results indicated that the GFRP bars were not severely damaged from two hours of heat exposure with the low elevated temperature exposure. (Hajiloo, H.; Green, M. F.; Noël, M.; Bénichou, N.; Sultan, M., 2019). Investigated the fire resistance of two full-scale GFRP RC slabs with only 40 mm of clear concrete cover and 200 mm of unexposed (cool) anchor zone at the ends. Both slabs endured 3 h under the standard fire. The slabs were loaded with a sustained load, which caused a moment equal to 45% of their ultimate flexural strength. The temperature reduces significantly in the unexposed zones, providing an adequate anchorage for the bars when almost the entire GFRP-to-concrete bond deteriorated in the exposed zone. Their results enabled an efficient, economic, and fire-safe application of GFRP reinforcement in concrete construction by reducing the concrete cover.

## Objectives

This investigation is a part of an extensive research program on the behavior of RC beams reinforced with GFRP under various loading conditions, which was carried out at the Helwan University. The objectives of this study were (1) to explore the feasibility and efficiency of using GFRP bars on RC beams under fire; (2) to investigate the influence of the GFRP reinforcement ratio on the concrete contribution to shear behavior of the specimens; and (3) to analyze the effect of fire on concrete shear capacity.

## Experimental Program

### *Materials*

The beams were constructed using normal-weight concrete (NWC) with a target compressive strength of 25 MPa after 28 days at room temperature. Table I gives the mixture proportions of the NWC used in this study. The actual compressive strengths of concrete,  $f'_c$ , were determined in accordance with (C39/C39M-18., 2018) from six concrete cylinders (100 x 200 mm) for the NWC. All cylinders were cured under identical conditions with the beams

**Table (1):**NWC mix proportions.

Concrete	
w/c	0.38
Water (Kg/m <sup>3</sup> )	210
Cement type	Portland cement
Cement content (Kg/m <sup>3</sup> )	382
Fine aggregate content (Kg/m <sup>3</sup> )	570
Coarse aggregate content (Kg/m <sup>3</sup> )	1200
Coarse aggregate size (mm)	10 to 20
Slump (mm)	85

The glass FRP bars employed in this study were manufactured and developed in Egypt. The bars were made of continuous longitudinal fibers impregnated in a thermosetting vinyl-ester resin with a typical fiber content of 73 %. Number 4 (12.7 mm diameter) bars with nominal cross-sectional areas of 129 mm<sup>2</sup> were used to reinforce the beam specimens in the longitudinal direction. Fig. 2 shows the stress-strain relationship of the GFRP bars as measured by standard tension tests in accordance with (ACI, 2004) (see Fig. 2). Fig. 3 illustrates the surface characteristics of the GFRP bars. In this investigation, the nominal values were selected for use in designing the beam specimens and in all analyses. The modulus of elasticity, ultimate tensile strength, and strain at rupture were estimated according to (ASTM, 2011). Table II presents the mechanical characteristics of the GFRP bars. Mild smooth steel bars of 8 mm diameter were used as top reinforcement to hold the stirrups behind the supports. Furthermore, one size of steel stirrups (8 mm diameter) was fabricated to use behind the supports for all the beams.

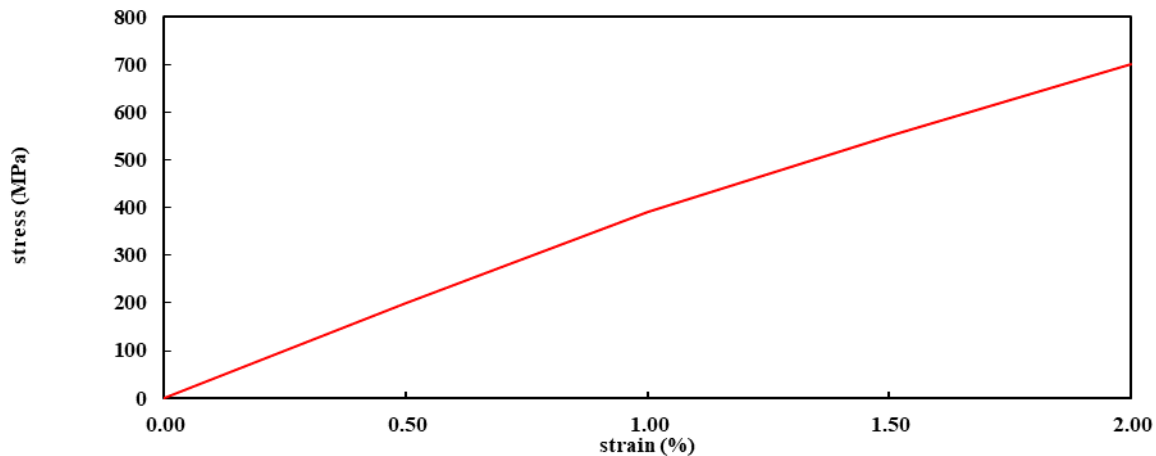
**Table (2):**Mechanical properties of the GFRP reinforcement

Bar type	GFRP bars
Bar size	No. 4
Diameter (mm)	12.7
$A_f$ $a$ (mm <sup>2</sup> )	129
$A_{im}$ $b$ (mm <sup>2</sup> )	138 ± 2
$E_f$ (GPa)	42.0 ± 1.5
$f_{fu}$ (MPa)	749 ± 27
$\epsilon_{fu}$ (%)	1.2

$a$  Nominal cross-sectional area.

$b$  Immersed cross-sectional area (measured).

Note: Properties calculated based on the nominal cross-sectional area.



**Fif (2):**Tensile test of GFRP bars.



**Fif (3):**Surface characteristics GFRP bars.

### ***Beam Design, Fabrication and Details***

Three RC beam specimens measuring  $150 \times 300$  mm were tested in this study, with a total span of 1700 mm. All beams were reinforced with GFRP bars. Two RC beams are exposed to fire, while the other one was used as a reference specimen. The influence of GFRP reinforcement ratio on the shear behavior was investigated by testing two beams reinforced longitudinally with No. 4 GFRP bars with reinforcement ratios of 2.3% and 1.0%. Two 8 mm steel bars were used as top reinforcement to hold the stirrups behind the supports. In addition, three stirrups 8 mm at each end were used to prevent anchorage failure. The details of the reinforcement and the tested beams are illustrated in Fig. 4. Each beam is identified with a label consisting of numbers and letters, beginning with B referring to the concrete member: Beam. The numbers 1 and 2 represent the longitudinal

reinforcement ratio, followed by the fire duration. Table III gives the test matrix of the beam specimens.

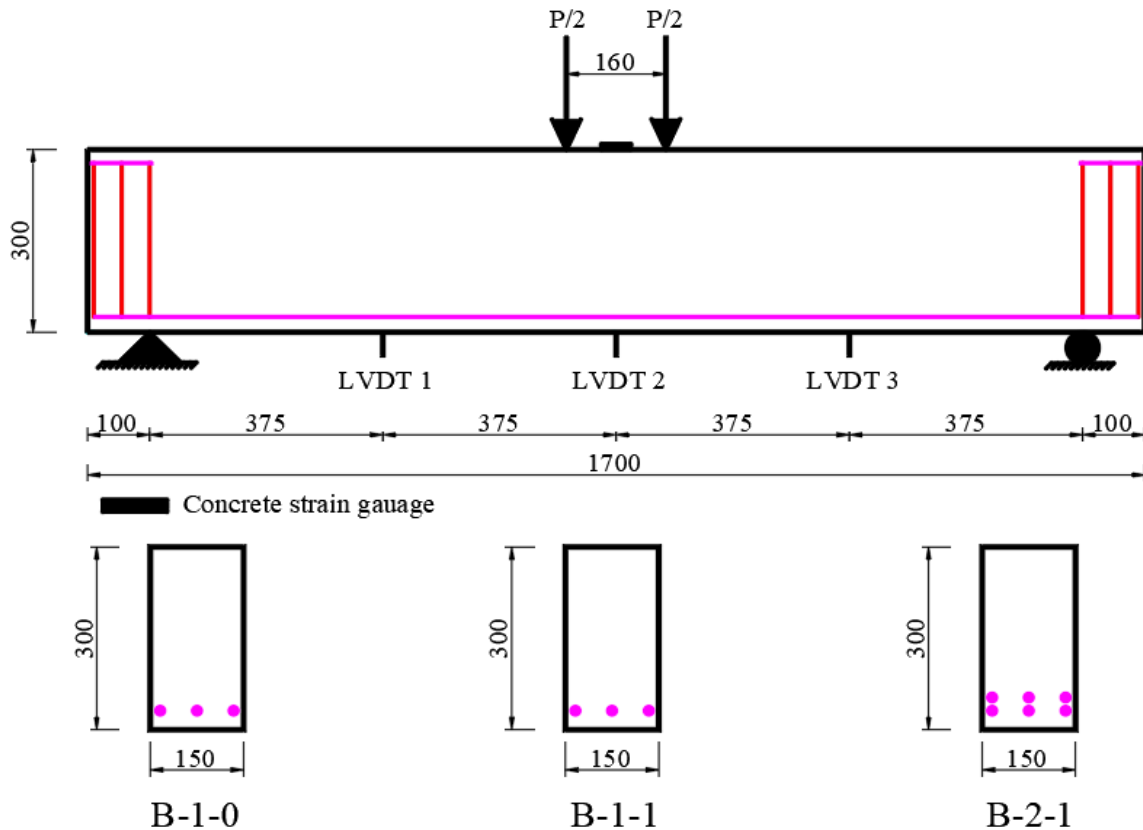


**Fig (4):** Dimensions, reinforcement details, and strain gauge locations of the test specimens (Note: dimensions in mm).

**Table (3):** Test matrix and details of the test specimens

ID	Reinforcing Material	$f_c$ (MPa)	$\rho_f$ (%)	Fire Duration (hr)
B-1-0	GFRP	25	1.0	0.0
B-1-1	GFRP	22	1.0	1.0
B-2-1	GFRP	22	2.3	1.0

### Instrumentation

Instrumentation of the beam specimens included three linear variable differential transducers (LVDTs) at different locations for deflection measurement. Two electric strain gauges with a gauge length of 60 mm were bonded to the compression surface of each specimen to measure the compressive concrete strains. Epoxy was used to attach the strain gauges to the compression beam surface after it was cleaned. Fig. 4 illustrates the instrumentation details of the test beams.



### ***Fire Exposure System***

A steel furnace with seven burners lined parallel to each other was used with dimension 2000 mm × 2000 mm × 600 mm. The furnace was heated to the required temperature, i.e. (500 °C) and then kept at this temperature for 2 h. The beams and cylinders were subjected to direct fire. The used regime for cooling the fire beams was air.

### ***Experimental Setup and Testing***

The beam specimens were subjected to four-point loading on a clear span length of 1500 mm (see Fig. 4). The beams were supported by two steel plates set on the supports. The load was applied with a 550 kN hydraulic jack in two phases. In the first phase, the load was applied in load-controlled mode at a rate of 2 kN/min up to the first crack. Then, the beam was loaded in load-controlled mode at a rate of 4 kN/min up to failure. The rigid steel beam was used to transfer two equal loads to the specimen. The load was removed from the test beams immediately after reaching the failure load.

## **Experimental Results and Discussions**

### ***Shear Failure Mode and Cracking***

The beam specimens clearly failed in shear failure mode before reaching their flexural capacities. Vertical flexural cracks were observed in all specimens perpendicular to the direction of the maximum principal stress induced by pure bending moment in the flexural span zone. Cracking outside the flexural span zone started as the load increased, similarly to flexural cracking. As more load was applied, the shear stress became more dominant and developed curving in both shear spans toward the loading points. Fig. 5 illustrates the typical failure mode of the tested beam specimens.

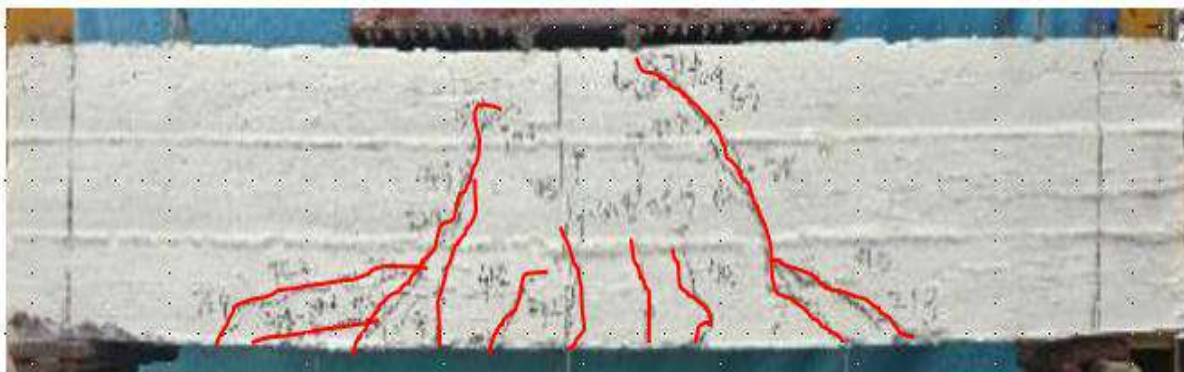


**Fig (5):** Typical crack pattern of beams

### Load–Deflection Behavior

This section presents the load–deflection curves of the test specimens in two groups to show the effect of test parameters on shear behavior, as shown in Figures 6 and 7. It can be observed that the relationship of load-deflection was bilinear. The first stage of the load-deflection curve for all beams exhibited a linear response until reaching flexural cracking. The second stage, after cracking, all specimens showed a significant loss of stiffness with a considerable increase in their point loads deflections. As shown in Fig. 6, the decreased stiffness varied because of the different reinforcement ratios. It can be noticed that increasing the reinforcement ratio resulted in higher stiffness and decreased its deflection at all stages of loading.

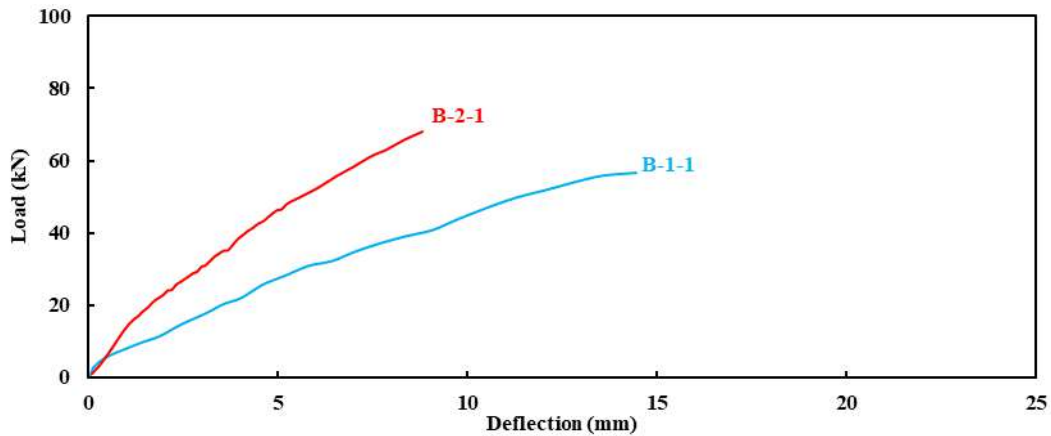


Fig (6):Load–deflection curves for beams at the same temperature (500 °C).

Fig. 7 shows that the stiffness of the RC beams decreased when the beams are exposed to fire at the same reinforcement ratio. In other words, B-1-0 was stiffer than B-1-1 at the same reinforcement ratio (1.0 %). In addition, the shear strength of the beam exposed to fire is 88 % of its room temperature shear strength.

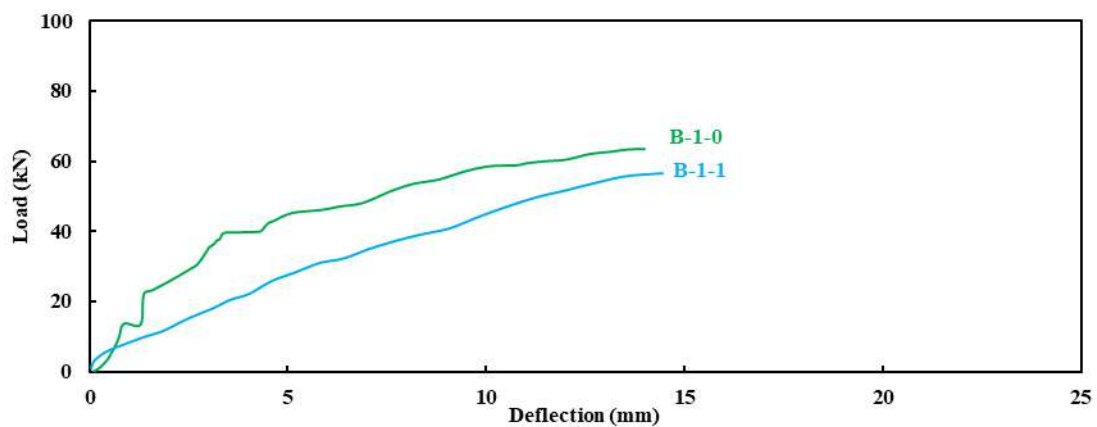
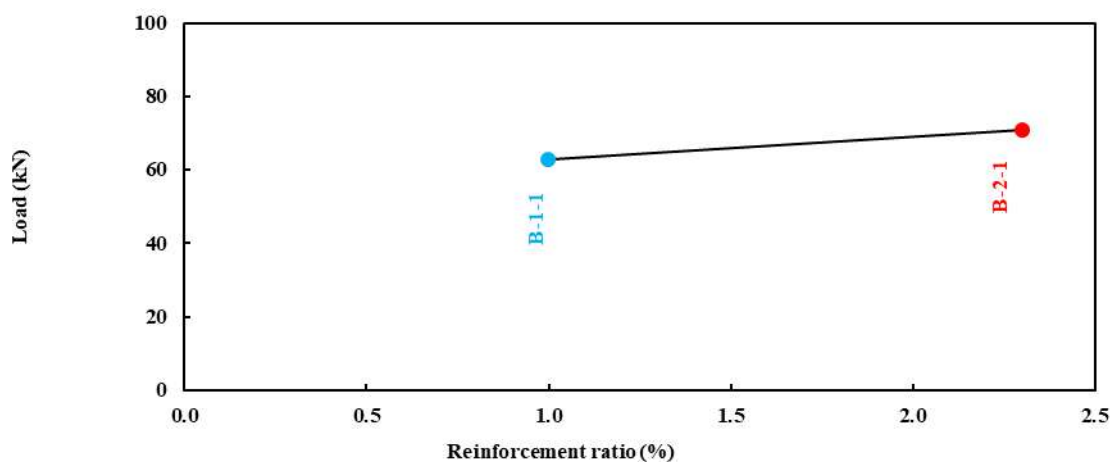


Fig (7):Load–deflection curves for beams at the same reinforcement ratio (1.0%).



### *Effect of the GFRP longitudinal reinforcement ratio*

Fig. 8 shows the influence of reinforcement ratio of the GFRP bars on the shear strength of the RC beams. The vertical axis represents the experimental load of the tested beams. While the horizontal axis represents the reinforcement ratio  $\rho$ . It was found that the shear strength increased as the reinforcement ratio was increased. The shear strength increased by 13.0 % when the longitudinal reinforcement ratio increased by 130 % (from 1.0 to 2.3 %). Moreover, cracking pattern for beams with higher amount of longitudinal reinforcement was more observed than that for beams with lower amount of longitudinal reinforcement.



**Fig (8):**Experimental load versus reinforcement ratio for GFRP reinforced beams.

### **Conclusions**

This paper presents the results of a research program to investigate the shear behavior of GFRP RC beams exposed to severe fires. The main remarks from the study can be drawn as follow:

1. Diagonal tension failure was the dominant failure mode of the GFRP RC beam specimens.
2. Increasing the reinforcement ratio resulted in higher stiffness and decreased its deflection at all stages of loading. The shear strength increased by 13.0 % when the longitudinal reinforcement ratio increased by 130 % (from 1.0 to 2.3 %).
3. The shear strength of the beam exposed to fire is 88 % of its room temperature shear strength at the same reinforcement ratio.
4. It is recommended to extend this study with more experimental works considering more samples to be tested for each test parameters.

---

## Acknowledgment

The authors thank the technical staff of the structural laboratory in the Department of Civil Engineering at Helwan University.

## References

- ACI, 4.-0. (2004). Guide test methods for fiber-reinforced polymers (FRPs) for reinforcing or strengthening concrete structures, ACI Committee 440. *American Concrete Institute, Farmington Hills, Michigan, USA.*
- American, C. I. (2015). Guide for the design and construction of concrete reinforced with FRP bars. *ACI 440.1R-15, Farmington Hills, MI.*
- ASCE-ACI, C. 4. (1998). Recent approaches to shear design of structures. *J. Struct. Eng., 10.1061/(ASCE) 0733-9445(1998)124:12(1375)*, 1375–1417.
- ASTM, D. (2011). Tensile properties of fiber reinforced polymer matrix composite bars. *ASTM International, West Conshohocken, PA.*
- ASTM. (2015). Standard test methods for fire tests of building construction and materials. ASTM E119. *West Conshohocken, PA: ASTM.*
- C39/C39M-18., A. (2018). Standard test method for compressive strength of cylindrical concrete specimens. *ASTM International, West Conshohocken, PA.*
- Canadian, S. A. (2019). Canadian highway bridge design code. *CSA S6-19, Rexdale, Ontario, Canada.*
- CSA, C. S. (2012). – Re-approved in 2017 –. Design and construction of building components with fiber reinforced polymers. *CSA S806-12. Rexdale, Ontario, Canada.*
- Gooranorimi, O., Claire, G., De Caso, F., Suaris, W., & Nanni, A. (2018). Post-fire behavior of GFRP bars and GFRP-RC slabs. *Journal of Materials in Civil Engineering, 30(3)*, 04017296.
- Hajiloo, H., Green, M. F., Noël, M., Bénichou, N., & Sultan, M. (2019). GFRP-reinforced concrete slabs: fire resistance and design efficiency. *Journal of Composites for Construction, 23(2)*, 04019009.
- Hajiloo, H., Green, M. F., Noël, M., Bénichou, N., & Sultan., M. (2017). Fire tests on full-scale FRP reinforced concrete slabs. *Compos. Struct. 179*, 705–719.
- Hajiloo, H.; Green, M. F.; Noël, M.; Bénichou, N.; Sultan, M. (2019). GFRP-reinforced concrete slabs: fire resistance and design efficiency. *Journal of Composites for Construction, 23(2)*, 04019009.
- MacGregor, J. G., & Wight, J. K. (2005). Reinforced concrete: Mechanics and design. 4th Ed. *Prentice-Hall, Upper Saddle River, NJ.*
- Nigro, E., G. Cefarelli, A., Bilotta, G. M., & Cosenza, E. (2011). Fire resistance of concrete slabs reinforced with FRP bars. Part I: Experimental investigations on the mechanical behavior. *Composites Part B 42 (6)*, 1739–1750.